ELSEVIER

On the significance of the surface states in isolated Al$_x$Ga$_{1-x}$N/GaN heterostructures

Juan Antonio Casao Pérez *

Dpto. Ingeniería Electrónica y Comunicaciones, Centro Politécnico Superior, Universidad de Zaragoza, C/María de Luna 3, 50012 Zaragoza, Spain

Abstract

The significance of the surface states in isolated Al$_x$Ga$_{1-x}$N/GaN heterostructures is investigated. A model based on a self-consistent solution of the Schrödinger, Poisson and charge balance equations is presented. The singular value decomposition is used to calculate the eigenstates of the real non-symmetric matrix which is obtained when a non-uniform mesh is used. The discontinuity of the spontaneous and piezoelectric polarization at the interface is taken into account. The results obtained for the 2DEG density and the surface potential agree well with theoretical and experimental data already published.
© 2005 Elsevier Ltd. All rights reserved.

Keywords: AlGaN/GaN; 2DEG; Surface states

1. Introduction

Two dimensional electron gas (2DEG) concentrations higher than 10^{13} cm^{-2} have been calculated and measured in heterostructures based on the AlGaN/GaN system [1–5]. This fact along with the good electron transport properties and good thermal conductivity of GaN, has resulted in the application of such heterostructure to the development of the electronics for high temperature and high power at microwave frequencies [6–8]. In the references mentioned above, the source of the 2DEG was supposed to be the donor doping (intentional or not) in the AlGaN layer or the donor surface states created at the AlGaN edge opposite the heterostructure.

In this article, the analyzed structure is assumed to be an Al$_x$Ga$_{1-x}$N layer pseudomorphically grown on a thick GaN buffer, at thermal equilibrium. The significance of the donor surface states is theoretically studied using a charge control model based on the self-consistent solution of the Schrödinger, Poisson and charge balance equations. A non-uniform mesh is used to discretize the equations and the singular value decomposition is used to calculate the eigenstates of the real non-symmetric matrix obtained. In Appendix A, a simple method to obtain an initial approximate solution of these equations is described. The calculated 2DEG density and surface potential are compared with simulated and experimental results recently published. Finally, Appendix B describes a method to estimate the minimum barrier width necessary to get a 2DEG density minimum [9]. This method is based on the equations of Appendix A.

2. Mathematical model

In the effective mass approximation, assuming the z axis to be along the [0 0 0 1] direction and without

---

* Tel.: +34 976761966; fax: +34 976762111.
E-mail address: casao@posta.unizar.es

considering the coupling between the electron motions along and perpendicular to the z axis, due to the position dependent effective mass $m(z)$; the Schrödinger equation for the conduction band becomes [10]

$$-\frac{\hbar^2}{2} \frac{d}{dz} \left(\frac{1}{m(z)} \frac{d\chi_n(z)}{dz} \right) + E_C(z) \cdot \chi_n(z) = \varepsilon_n \cdot \chi_n(z) \qquad (1)$$

where $E_C(z) = E_{cr} - q\psi(z) + \Delta E_C(z) + qV_{xc}(z)$ is the band conduction energy, E_{cr} is a reference constant, $\Delta E_C(z)$ is the conduction band discontinuity, $\psi(z)$ is the self-consistent electrostatic potential solution of the Poisson equation and $V_{xc}(z)$ is the exchange-correlation potential [11]. The finite difference method has been used to solve the Schrödinger equation. In the $Al_xGa_{1-x}N$, $-LSLG \leqslant z \leqslant 0$ (Length Semiconductor Large Gap), the discretization is uniform, with a step denoted by h_uni; but in the GaN, $0 < z \leqslant LSSG$ (Length Semiconductor Small Gap), the jth and $(j + 1)$th steps are related by $h_{j+1} = h_j(1 + f)$, being f a constant much smaller than one [12]. If the ith node corresponds to $z = 0$, at the interface between the $Al_xGa_{1-x}N$ and GaN, from Eq. (1) it follows that

$$\chi_{n,i+1} \left(\frac{1}{h_i + h\_uni} \right) \cdot \frac{1}{h_i} (1 + \delta_m) - \chi_{n,i} \left(\frac{1}{h_i + h\_uni} \right)$$
$$\cdot \left[\frac{1}{h_i} (1 + \delta_m) + \frac{2}{h\_uni} \cdot \delta_m \right] + \chi_{n,i-1} \left(\frac{1}{h_i + h\_uni} \right)$$
$$\cdot \frac{2}{h\_uni} \cdot \delta_m + \frac{2m_A}{\hbar^2} [-E_{C,i} + \varepsilon_n] \cdot \chi_{n,i} = 0 \qquad (2)$$

where $\delta_m = m^{GaN}/m^{AlGaN} = m_A/m_B(x)$ and x is the composition of the $Al_xGa_{1-x}N$. Using this discretization, the step size in the GaN region near to $z = 0$, where the 2DEG takes significant values and the electrostatic potential varies quickly, can be made very small; while in the GaN region far away from $z = 0$, where the potential varies slowly, the step size can be made higher. So, the following matrix equation can be obtained

$$S1 \cdot \bar{\chi}_n = \lambda_n \cdot \bar{\chi}_n \qquad (3)$$

in which, because of the non-uniform discretization, the $NX \times NX$ square matrix $S1$ is tridiagonal and non-symmetric, NX is the number of nodes considered in $-LSLG \leqslant z \leqslant LSSG$ and $\bar{\chi}_n$ is the normalized wave function with respect to LSSG. The node $i = 1$ corresponds to $z = -LSLG$, and $i = NX$ with $z = LSSG$; and it has been considered that $\chi_{n,i=0} = \chi_{n,i=(NX+1)} = 0$, $h_{i=0} = h_{i=1}$ and $h_{i=NX} = h_{i=(NX-1)}$. First, using numerical recipes given in [13] the eigenvalues of $S1$ λ_n, $n = 1, 2, \ldots, NX$, are computed. For the eigenvalue in which we are interested, the following homogeneous linear system is formed

$$(S1 - \lambda_n \cdot I) \cdot \bar{\chi}_n = S2_n \cdot \bar{\chi}_n = 0 \qquad (4)$$

where I is the unity matrix. By construction, $S2_n$ is singular for every n. Now, the singular value decomposi-

tion of $S2_n$ is computed, so that $S2_n$ can be written as [13]

$$S2_n = U_n \cdot \begin{pmatrix} w_{n,1} & 0 & \ldots & 0 & 0 \\ 0 & w_{n,2} & \ldots & 0 & 0 \\ \ldots & \ldots & \ldots & \ldots & \ldots \\ 0 & 0 & \ldots & \ldots & 0 \\ 0 & 0 & \ldots & 0 & w_{n,NX} \end{pmatrix} \cdot V_n^T \qquad (5)$$

where only one of the $w_{n,k}$, $k = 1, 2, \ldots, NX$, is equal to zero; say $w_{n,k0} = 0$ (non-degenerate eigenvalues are assumed). Also by construction, the k_0th column of the matrix V_n constitutes an orthonormal vector belonging to the nullspace of the matrix $S2_n$; that is, the nth eigenvector corresponding to the eigenvalue λ_n. Since the wave function $\chi(z)$ is normalized to unity

$$\int_{-LSLG}^{LSSG} [\chi_n(z)]^2 \cdot dz = \int_{-\overline{LSLG}}^{1.0} [\bar{\chi}_n(z)]^2 \cdot d\bar{z} = 1.0$$
$$= \sum_{i=1}^{(NX-1)} [\bar{\chi}_{n,i}]^2 \cdot \bar{h}_i = \sum_{i=1}^{NX} (V_{n,i,k0})^2 \qquad (6)$$

Therefore,

$$\bar{\chi}_{n,i} = \frac{V_{n,i,k0}}{\sqrt{\bar{h}_i}}, \quad i = 1, 2, \ldots, (NX - 1)$$
$$\bar{\chi}_{n,NX} = V_{n,NX,k0} = 0 \qquad (7)$$

The quantum electronic concentration is given by

$$n_{2D}(z) = \frac{m_A kT}{\pi \hbar^2} \cdot \sum_{n=1}^{\infty} [\chi_n(z)]^2 \cdot \ln \left\{ 1 + \exp \left[\frac{E_F - \varepsilon_n}{kT} \right] \right\} \qquad (8)$$

with E_F the Fermi level. The Poisson equation is written as

$$\frac{d}{dz} \left(\varepsilon(z) \frac{d\psi(z)}{dz} \right) = -\rho(z) + \frac{dP}{dz} \qquad (9)$$

where the $\varepsilon(z) = \varepsilon_B(x)$ for the $Al_xGa_{1-x}N$ and $\varepsilon(z) = \varepsilon_A$ for the GaN, $P(z)$ is the spontaneous and piezoelectric polarization and

$$\rho(z) = q \cdot \lfloor N_d^+(z) - N_a^-(z) - n_{3D}(z) - n_{2D}(z) + p_{3D}(z) \rfloor,$$
$$- LSLG \leqslant z \leqslant LSSG \qquad (10)$$

The discretized Poisson equation at $z = 0$ (ith node), is expressed as

$$\varepsilon_A \left(\frac{\psi_{i+1} - \psi_i}{h_i} \right) - \varepsilon_B \left(\frac{\psi_i - \psi_{i-1}}{h\_uni} \right)$$
$$= - \left(\frac{h\_uni}{2} \cdot \rho_{i-1/2} + \frac{h_i}{2} \cdot \rho_{i+1/2} \right)$$
$$+ P(GaN) - P(AlGaN) \qquad (11)$$

$p_{3D}(z)$ is computed using the Fermi–Dirac integral $F_{1/2}$ $(\eta_V(z))$, with $\eta_V(z) = (E_V(z) - E_F)/kT$. In order to calculate $n_{3D}(z)$, the method exposed in [14,15] has been used;

in which the GaN is divided in two regions: in the first one, $E_C(z) \leqslant E_b$ being E_b an energy level which has to be carefully chosen, so that

$$n_{3D}(z) = \frac{2N_C^{\text{GaN}}}{\sqrt{\pi} \cdot kT} \int_{E_b}^{\infty} \frac{\sqrt{\frac{E-E_C(z)}{kT}} - \sqrt{\frac{E_b-E_C(z)}{kT}}}{1 + \exp\left[\frac{E-E_F}{kT}\right]} dE \quad (12)$$

and in the second one, $E_C(z) \geqslant E_b$, so that $n_{3D}(z)$ is given by the familiar Fermi–Dirac integral $F_{1/2}(\eta_C(z))$, with $\eta_C(z) = (E_F - E_C(z))/kT$. E_b has been made equal to the quantum level $E_{n=4}$. Therefore, only the first three bound states have been taken into account. Also, E_b has been assumed to be a few times kT above E_F; consequently, the classical electrons in GaN have been considered non-degenerated. Then, Eq. (12) can be simplified; in particular, the first term in Eq. (12) can be written as

$$\frac{2N_C^{\text{GaN}}}{\sqrt{\pi} \cdot kT} \cdot \int_{E_b}^{\infty} \frac{\sqrt{\frac{E-E_C(z)}{kT}}}{1 + \exp\left[\frac{E-E_F}{kT}\right]} dE = N_C^{\text{GaN}} \cdot \frac{2}{\sqrt{\pi}}$$

$$\cdot \int_{x_b(z)}^{\infty} x^{1/2} \cdot \exp[-x + \eta_C(z)] dx \quad (13)$$

where $x_b(z) = (E_b - E_C(z))/kT$. The $Al_xGa_{1-x}N$ has been supposed to be undoped, and the GaN with a non-intentional acceptor doping $N_A^{\text{GaN}} = 1.0 \times 10^{16} \text{ cm}^{-3}$ and an ionization energy of 50 meV. The source of the 2DEG has been assumed to be the existence of surface donor states in the edge $z = -LSLG$ of the $Al_xGa_{1-x}N$; with a concentration $N_{SD} = 1.5 \times 10^{13} \text{ cm}^{-2}$ and an ionization energy $E_{SD} = 1.4$ or 1.5 eV [1,3,16–18]. Using Fermi–Dirac statistics, the ionized surface donor concentration N_{sd}^+ can be expressed as

$$N_{sd}^+ = \frac{N_{SD}}{1 + g_D \exp\left[\frac{E_F - E_{sd}}{kT}\right]} \quad (14)$$

with $E_{sd} = E_C(z = -LSLG) - E_{SD}$ and $g_D = 2$. In this article, the heterostructure at thermal equilibrium has been studied. Therefore, the charge balance equation has been solved simultaneously with the Poisson and Schrödinger equations. Such an equation is

$$N_{sd}^+(\psi(z = -LSLG)) - \frac{m_A kT}{\pi \hbar^2} \sum_{n=1}^{3} \ln\left\{1 + \exp\left[\frac{E_F - \varepsilon_n}{kT}\right]\right\}$$

$$- \int_0^{LSSG} [N_a^-(z) + n_{3D}(z) - p_{3D}(z)] \cdot dz = 0 \quad (15)$$

The Fermi level has been taken as reference, $E_F = 0$. The boundary condition $E_C(z = LSSG) = E_{CA}$, where E_{CA} is the conduction band level in the neutral GaN, has been forced; then, $E_{CA} = E_{cr} - q\psi(z = LSSG)$. As a reference for the potential, $\psi(z = LSSG) = 0.0$ has been chosen, and the boundary condition $d\psi/dz|_{z=LSSG} = 0.0$ has been imposed. With these conditions the electrostatic potential at $z = -LSLG$ is an unknown to be determined by

the self-consistent solution of the Poisson, Schrödinger and charge balance equations.

The equations that determine the physical parameters of the GaN together with $m_B(x)$, $\varepsilon_B(x)$, $E_{gB}(x)$, $P_{\text{spon,B}}(x)$, $P_{\text{piez,B}}(x)$ and $\Delta E_C(x)$, have been taken from Refs. [2,4,19].

The method based on a predictor–corrector approach reported in [20], has been used. An initial solution obtained from the simplified equations shown in Appendix A is used to begin the iterative scheme, until convergence is reached.

3. Results and discussion

Fig. 1 shows the 2DEG density calculated as a function of the $Al_xGa_{1-x}N$ barrier width, with x as a parameter and $T = 300$ K. For a fixed x, these graphs show that there exits a threshold barrier thickness below which the 2DEG is not formed. For high LSLG, the majority of the surface states are ionized and, because of the charge conservation, the 2DEG density reaches its saturation value $n_{S,sat}$, given by $N_{SD} = n_{S,sat} + N_{dep}$, where N_{dep} is a 2D equivalent acceptor doping in the channel (see Appendix A). Unlike Refs. [5,18], in these simulations N_{SD} and E_{SD} are fixed and the surface potential $E_C(-LSLG)$ is determined once the iterative scheme has converged to the solution. So, with LSLG = 300 Å and $x = 0.3$, a value of 1.497 eV for $E_C(-LSLG)$ has been reached after convergence. This value is in agreement with the 1.46 eV supposed in Ref. [5], when an approximate value of $1.5 \times 10^{13} \text{ cm}^{-2}$ is reached for N_{SD} after convergence. The results shown in Fig. 1 match both, the theoretical [1,2,5,17,18] and the experimental [3,16,21] results, recently published. For $x = 0.4$ and $x = 0.35$ and in all figures, the only results shown are those in which $E_C(-LSLG)$ is less than or
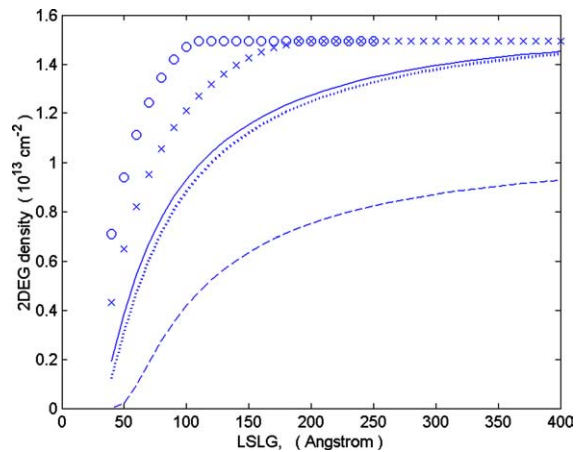

Fig. 1. Calculated 2DEG density as a function of the barrier width with $x = 0.2$ (dashed), 0.3 (solid), 0.35 (×) and 0.4 (○). Also the curve with $x = 0.3$, and $E_{SD} = 1.5$ eV is shown (dotted line).

equal to 3.65 eV; therefore the effect of the holes in the $Al_xGa_{1-x}N$ can be ignored. These simulations are essentially different from those shown in Refs. [5,18], because when N_{SD} remains fixed in every simulation; for (a) $x = 0.4$ and LSLG $\geqslant 110$ Å and, (b) $x = 0.35$ and LSLG $\geqslant 190$ Å; the 2DEG density takes its value of saturation $n_{S,sat} \approx 1.494 \times 10^{13}$ cm^{-2}, the electric field in the $Al_xGa_{1-x}N$ is constant, independent of LSLG and approximately given by (from Eqs. in Appendix A):

$$F(0^-) = (1/\varepsilon_B) \cdot [N_{SD} - P(Al_xGa_{1-x}N) + P(GaN)] \tag{16}$$

Consequently, for LSLG beyond those values, the 2DEG density and its energetic distribution remain invariable and, an increase in LSLG only produces a proportional increase in $E_C(-LSLG)$. A simulation with $x = 0.3$ and $E_{SD} = 1.5$ eV is included in Fig. 1 (dotted line), showing a slight decrease in the 2DEG density; the higher LSLG is the lower this decrease is. Also, simulations with an acceptor doping in the GaN higher than the initial value of 1.0×10^{16} cm^{-3} and equal to 10^{18} cm^{-3} were performed, producing a important decrease in the 2DEG density of 0.56×10^{12} cm^{-2}, practically independent of the value of LSLG and x considered [22].

In Fig. 2, the conduction band edge, the quantum electron concentration and the first three wave functions are shown for LSLG = 300 Å and $x = 0.3$. In this case, $E_b = \varepsilon_4$ is 2.8 times kT, so that the assumption of non-degenerate 3D electrons in GaN is reasonable. The calculated 2DEG density is 1.39×10^{13} cm^{-2} and the energy levels are $\varepsilon_1 = -125$ meV, $\varepsilon_2 = 1.0$ meV and $\varepsilon_3 = 46$ meV; as a result, the 85.3% of the electrons are in the first level, the 12.0% in the second and the 2.7% in the third. In [5] a 2DEG density equal to 1.5×10^{13} cm^{-2} is obtained for these values of LSLG and x; the difference between the two values being

caused by the use of material parameters slightly different, mainly in the polarization.

From Fig. 3, for a fixed x, it can be seen that the surface potential increases very slowly with LSLG if the barrier width remains below the value for which the 2DEG reaches saturation. For example, with $x = 0.3$ $E_C(-LSLG)$ varies from 1.41 eV to 1.48 eV when LSLG goes from 60 Å to 250 Å. Such variation corresponds with an important increase in the 2DEG density which varies from 0.54×10^{13} cm^{-2} to 1.35×10^{13} cm^{-2}. The curves with $x = 0.35$ and $x = 0.4$ clearly show that, once the 2DEG density is saturated, $E_C(-LSLG)$ increase linearly with LSLG; and the slope, i.e., the electric field at the $Al_xGa_{1-x}N$ is higher, the higher x is; as can be deduced from Eq. (16). This behaviour is more easily appreciated in Fig. 4 where the 2DEG density versus $E_C(-LSLG)$ is presented for $x = 0.2$ (+), 0.3 (●) and

Fig. 3. Calculated $E_C(-LSLG)$ as a function of the barrier width with $E_{SD} = 1.4$ eV and, $x = 0.2$ (dashed line), 0.3 (solid), 0.35 (×) and 0.4 (○).
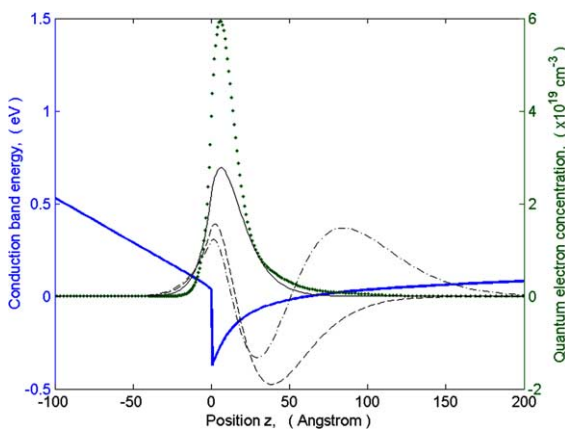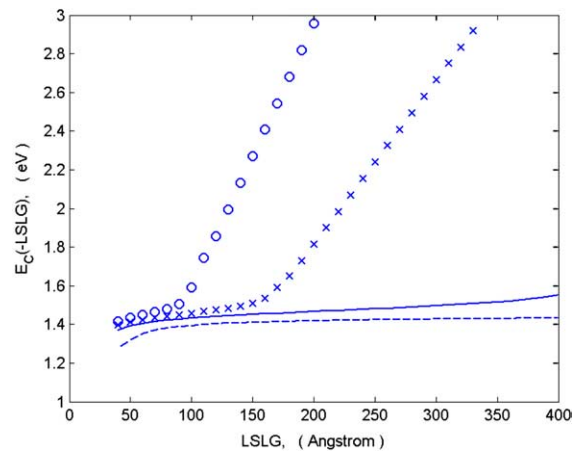

Fig. 2. Calculated conduction band edge (thick solid line), quantum electron concentration $n_{2D}(z)$ (dot line) and the first wave function (solid), second (dashed) and third (dot-dashed); with LSLG = 300 Å and $x = 0.3$. The scale for the wave functions is arbitrary.
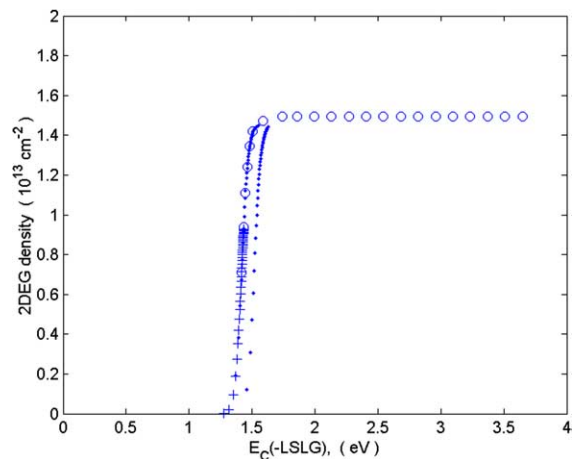

Fig. 4. Calculated 2DEG density versus $E_C(-LSLG)$ for an undoped $Al_xGa_{1-x}N$/GaN structure with $x = 0.2$ (+), 0.3 (●) and 0.4 (○). Also the curve with $x = 0.3$ and $E_{SD} = 1.5$ eV (●, right) is shown.

0.4 (○) and; for every x, LSLG varies from 40 Å to 400 Å. This curve is completely different from the one shown in [18], since in our simulations, n_S increases due to the fact that the barrier width increases with fixed N_{SD} and E_{SD}. With E_{SD} fixed, when the 2DEG density varies significantly, the surface potential remains near but below E_{SD}, and a small increase in $E_C(-\text{LSLG})$ produces a remarkable increase in the 2DEG density. It is clear that the points of the three curves $x = 0.2$, 0.3 and 0.4, are located on different overlapping sections of a specific curve; and the value of x only determines the section which is going to be obtained. The graph with $x = 0.3$ and $E_{SD} = 1.5$ eV is also shown (●, right), clearly indicating that, while the 2DEG density is not saturated, $E_C(-\text{LSLG})$ is pinned by the donor surface states. Also from Fig. 3, a linear relationship $E_C(-\text{LSLG}) = a \cdot x + b$ eV between the surface potential and the composition x can be obtained. However, typical values of a and b are 0.44 and 1.28 respectively; which differ significantly from those given in [2] for a Ni Schottky barrier, where $q\phi_B = 1.3 \cdot x + 0.84$. This discrepancy indicates that the metal work function play a main role in the formation of the Schottky barrier; and the Fermi level in a Schottky union is not pinned by the surface states of the $Al_xGa_{1-x}N$.

4. Conclusions

To sum up, the significance of the donor surface states in the $Al_xGa_{1-x}N$/GaN heterostructure has been investigated. Since the heterostructure is assumed to be isolated, the Schrödinger, Poisson and charge balance equations have to be solved simultaneously. A method based on the singular value decomposition to calculate the eigenvectors of the Schrödinger equation has been used. The influence of different physical parameters such as the barrier width, the composition x, the ionization energy of the surface states, and an acceptor doping in the GaN on the 2DEG density and the surface potential has been exposed; and the results obtained are compared with those published in the technical literature.

Appendix A

The approximate solution considers that part of the electrons transferred to the GaN occupy acceptors impurity states in the interval $0 \leqslant z \leqslant l_a$, with l_a given in [10]; and for $z < l_a$ the GaN remains neutral. Therefore, the integral in Eq. (15) is reduced to $N_{dep} = N_A^{GaN} \cdot l_a$. Then, the charge balance equation simplifies to

$$\frac{N_{SD}}{1 + g_D \exp\left[\frac{-E_{cr} + q\psi(-\text{LSLG}) - \Delta E_C + E_{SD}}{kT}\right]} - (n_S + N_{dep}) = 0$$

(A.1)

where n_S is the bidimensional electron density. From the Poisson equation and the boundary conditions, it is easy to obtain the following equations:

$$\varepsilon_A \cdot F(0^+) - \varepsilon_B \cdot F(0^-) = P(\text{AlGaN}) - P(\text{GaN}) \quad \text{(A.2a)}$$

$$F(0^+) = (q/\varepsilon_A) \cdot (n_S + N_{dep}) \quad \text{(A.2b)}$$

$$\psi(-\text{LSLG}) = \psi(0) + F(0^-) \cdot \text{LSLG} \quad \text{(A.2c)}$$

where $F(0^-)$ and $F(0^+)$ are the electric field at $z = 0^-$ and $z = 0^+$ respectively. As an approximate solution for the Schrödinger equation, all the electrons are assumed to be in the lowest energy level of the quantum well, whose energy E_1 is given by the infinite triangular quantum well approximation, with an effective electric field $F_{eff} = (q/\varepsilon_A) \cdot (0.5 \cdot n_S + N_{dep})$. Then ($E_F = 0$),

$$n_S = \frac{m_A kT}{\pi\hbar^2} \cdot \ln\left\{1 + \exp\left[-\frac{E_{cr} - q\psi(0) + E_1}{kT}\right]\right\} \quad \text{(A.3)}$$

The last five equations with the five unknowns n_S, $\psi(0)$, $\psi(-\text{LSLG})$, $F(0^-)$ and $F(0^+)$, can be reduced to one nonlinear equation in n_S, which is solved numerically. The wave function of the lowest state is assumed to be the first function of Fang and Howard [10]. With the $n_{2D}(z)$ obtained using Eq. (8), the Poisson equation is solved again analytically to obtain an initial solution for the electrostatic potential $\psi(z)$.

Appendix B

The five equations in Appendix A can be used to obtain the minimum width of $Al_xGa_{1-x}N$ necessary to make the quantum well exist with a minimum 2DEG density, specified by $n_{S,min}$. On quantitative terms, such $n_{S,min}$ can be defined by the condition that the lowest energy level is equal to the Fermi level, i.e., $\varepsilon_1 = E_F$. As a result, $n_{S,min} = (m_A kT/\pi\hbar^2) \cdot \ln(2)$ m^{-2}; which is approximately equal to 1.7×10^{12} cm^{-2}. From (A.1)–(A.3), the following equation can be reached for the minimum width

$$\text{LSLG}_{min} = \frac{1}{qF(0^-)}\left[\Delta E_C - E_{SD} + kT \ln \right.$$
$$\left. \times \left\{\frac{1}{g_D}\left(\frac{N_{SD}}{n_{S,min} + N_{dep}} - 1.0\right)\right\} - E_1(n_{S,min})\right]$$

(B.1)

Eq. (B.1) is similar to that published in [16] for the critical barrier thickness, but more complete. An analogous result can be obtained if the origin of the 2DEG is assumed to be the donor doping N_D in the Al_x-$Ga_{1-x}N$, and $q\phi_B$ is assumed to be a function of the composition x, as in [9]. Then, the following equation is reached

$$0 = -\frac{q}{2\varepsilon_B} N_D \cdot \mathrm{LSLG}_{\min}^2 + F(0^-) \cdot \mathrm{LSLG}_{\min} + \phi_B$$

$$- \frac{\Delta E_C}{q} + \frac{E_1(n_{S,\min})}{q} \tag{B.2}$$

The results obtained from Eq. (B.2) are broadly in agreement with those given in [9], obtained by self-consistently solving of the Poisson and Schrödinger equations.

References

[1] Hsu L, Walukiewicz W. Effects of piezoelectric field on defect formation, charge transfer, and electron transport at GaN/Al$_x$Ga$_{1-x}$N interfaces. Appl Phys Lett 1998;73(3):339–41.

[2] Ambacher O, Smart J, Shealy JR, Weimann NG, Chu K, Murphy M, et al. Two-dimensional electron gases induced by spontaneous and piezoelectric polarization charges in N- and Ga-face AlGaN/GaN heterostructures. J Appl Phys 1999;85(6):3222–33.

[3] Smorchkova IP, Elsass CR, Ibbetson JP, Vetury R, et al. Polarization-induced charge and electron mobility in AlGaN/GaN heterostructures grown by plasma-assisted molecular-beam epitaxy. J Appl Phys 1999;86(8):4520–6.

[4] Zhang Y, Singh J. Charge control and mobility studies for an AlGaN/GaN high electron mobility transistor. J Appl Phys 1999;85(1):587–94.

[5] Jogai B. Free electron distribution in AlGaN/GaN heterojunction field-effect transistors. J Appl Phys 2002;91(6):3721–9.

[6] Chumbes EM, Schremer AT, Smart JA, Wang Y, et al. AlGaN/GaN high electron mobility transistors on Si (111) substrates. IEEE Trans Electron Dev 2001;ED-48:420–6.

[7] Sacconi F, Di Carlo A, Lugli P, Morkoç H. Spontaneous and piezoelectric polarization effects on the output characteristics of AlGaN/GaN heterojunction modulation doped FETs. IEEE Trans Electron Dev 2001;ED-48:450–7.

[8] Morkoç H, Di Carlo A, Cingolani R. GaN-based modulation doped FETs and UV detectors. Solid State Electron 2002;46:157–202.

[9] Kalafi M, Asgari A. The behaviour of two-dimensional electron gas in GaN/Al$_x$Ga$_{1-x}$N/GaN heterostructures with very thin Al$_x$Ga$_{1-x}$N barriers. Physica E 2003;19:321–7.

[10] Bastard G. Wave mechanics applied to semiconductor heterostructures. Paris: Les editions de Physique; 1988.

[11] Hedin L, Lundqvist BI. J Phys C 1971;4:2064.

[12] Selberherr S. Analysis and simulation of semiconductor devices. Wien: Springer-Verlag; 1984.

[13] Press WH, Teukolsky SA, Vetterling WT, Flanery BP. Numerical recipes in C. The art of scientific computing. 2nd ed. Cambridge University Press; 1992.

[14] Wang T, Hsieh C-H. Numerical analysis of nonequilibrium electron transport in AlGaAs/InGaAs/GaAs pseudomorphic MODFET's. IEEE Trans Electron Dev 1990;ED-37(9):1930–8.

[15] Takano C, Yu Z, Dutton RW. A nonequilibrium one-dimensional quantum-mechanical simulation for AlGaAs/GaAs HEMT structures. IEEE Trans Comput-Aided Des 1990;9(11):1217–24.

[16] Ibbetson JP, Fini PT, Ness KD, DenBaars SP, Speck JS, Mishra UK. Polarization effects, surface states, and the source of electrons in AlGaN/GaN heterostructure field effect transistors. Appl Phys Lett 2000;77(2):250–2.

[17] Hsu L, Walukiewicz W. Effect of polarization fields on transport properties in AlGaN/GaN heterostructures. J Appl Phys 2001;89(3):1783–9.

[18] Jogai B. Influence of surface states on the two-dimensional electron gas in AlGaN/GaN heterojunction field effect transistors. J Appl Phys 2003;93(3):1631–5.

[19] Ambacher O, Majewski J, Miskys C, Link A, Hermann M, Eickhoff M, et al. Pyroelectric properties of Al(In)GaN/GaN hetero- and quantum well structures. J Phys: Condens Matter 2002;14:3399–434.

[20] Trellakis A, Galick AT, Pacelli A, Ravaioli U. Iteration scheme for the solution of the two-dimensional Schrödinger–Poisson equations in quantum structures. J Appl Phys 1997;81(12):7880–4.

[21] Smorchkova IP, Chen L, Mates T, et al. AlN/GaN and (Al,Ga)N/AlN/GaN two-dimensional electron gas structures grown by plasma-assisted molecular-beam epitaxy. J Appl Phys 2001;90(10):5196–201.

[22] Shur MS. GaN based transistors for high power applications. Solid State Electron 1998;42:2131–8.